800610

NUREG/CR-1789
ORNL/NUREG/TM-399

OAK RIDGE NATIONAL LABORATORY

UNION CARBIDE

ORTURB: A Digital Computer Code to Determine the Dynamic Response of the Fort St. Vrain Reactor Steam Turbines

J. C. Conklin

Prepared for the U.S. Nuclear Regulatory Commission
Office of Nuclear Regulatory Research
Under Interagency Agreements DOE 40-551-75 and 40-552-75

OPERATED BY
UNION CARBIDE CORPORATION
FOR THE UNITED STATES
DEPARTMENT OF ENERGY

Printed in the United States of America. Available from
National Technical Information Service
U.S. Department of Commerce
5285 Port Royal Road, Springfield, Virginia 22161

Available from

GPO Sales Program
Division of Technical Information and Document Control
U.S. Nuclear Regulatory Commission
Washington, D.C. 20555

NUREG/CR-1789
ORNL/NUREG/TM-399
Dist. Category R8

Contract No. W-7405-eng-26

14

Engineering Technology Division

ORTURB: A DIGITAL COMPUTER CODE TO DETERMINE THE DYNAMIC RESPONSE OF THE FORT ST. VRAIN REACTOR STEAM TURBINES

J. C. Conklin 14

Manuscript Completed — March 5, 1981
Date Published — March 1981

NOTICE This document contains information of a preliminary nature. It is subject to revision or correction and therefore does not represent a final report.

Prepared for the
U.S. Nuclear Regulatory Commission
Office of Nuclear Regulatory Research
Under Interagency Agreements DOE 40-551-75 and 40-552-75

NRC FIN No. B0122

Prepared by the
OAK RIDGE NATIONAL LABORATORY
Oak Ridge, Tennessee 37830
operated by
UNION CARBIDE CORPORATION
for the
DEPARTMENT OF ENERGY

CONTENTS

	Page
LIST OF SYMBOLS	v
ABSTRACT	1
1. INTRODUCTION	1
2. HIGH-PRESSURE TURBINE SIMULATION	5
3. REGENERATIVE INTERMEDIATE- AND LOW-PRESSURE TURBINE SIMULATIONS	9
4. FEEDWATER HEATER SIMULATION	13
5. CONTROL	21
6. RESULTS	23
REFERENCES	27
APPENDIX A. INPUT REQUIREMENTS	29
APPENDIX B. OUTPUT	33

LIST OF SYMBOLS

Nomenclature

A	a constant
A_f	cross-sectional flow area
C_p	specific heat
g_c	gravitational constant
h	specific enthalpy
k	isentropic exponent
K_{ex}	shape-loss constant for extraction flow
M	mass
P	pressure
T	temperature
UA	overall heat transfer coefficient multiplied by heat transfer area
v	velocity
V	volume
W	flow
W_{ex}	extraction steam flow
ν	specific volume
ρ	density
ΔP	pressure drop

Subscripts used in feedwater heater modeling (Eqs. 9 through 34)

A	halfway
C	condensing
DC	drain cooler
f	flash
fg	flash from liquid to vapor
FC	feedwater in drain-cooler section
FW	feedwater
FE	feedwater in vapor section
i	feedwater heater inlet
Q	outlet
s	extraction flow

sat	saturation conditions
SH	superheat
v	vapor
ℓ	liquid
ϕ	feedwater heater outlet

OBTURB: A DIGITAL COMPUTER CODE TO DETERMINE THE DYNAMIC RESPONSE OF THE FORT ST. VRAIN REACTOR STEAM TURBINES

J. C. Conklin

ABSTRACT

ORTURB is a computer code written specifically to calculate the dynamic behavior of the Fort St. Vrain (FSV) High-Temperature Gas-Cooled Reactor (HTGR) steam turbines. The ORTURB program can be independently exercised but is intended to be used in the overall FSV plant simulator code ORTAP currently under development at Oak Ridge National Laboratory.

ORTURB uses a relationship derived for ideal gas flow in an iterative fashion that minimizes computational time to determine the pressure and flow in the FSV steam turbines as a function of plant transient operating conditions. An important computer modeling characteristic, unique to FSV, is that the high-pressure turbine exhaust steam is used to drive the reactor core coolant circulators prior to entering the reheater.

A feedwater heater dynamic simulation model utilizing seven state variables for each of the five heaters completes the ORTURB computer simulation of the regenerative Rankine cycle steam turbines.

1. INTRODUCTION

The Nuclear Regulatory Commission (NRC) Division of Reactor Safety Research has funded a research program at Oak Ridge National Laboratory (ORNL) since July 1974 to analyze the response of the Fort St. Vrain High-Temperature Gas-Cooled Reactor (HTGR) plant to transient conditions (Fig. 1). Owned and operated by Public Service Company of Colorado, this demonstration reactor is the nation's only HTGR and was designed and built by the General Atomic Company of San Diego, California, with financial assistance from the U.S. Atomic Energy Commission.

The ORTAP code[1] was developed under sponsorship from this research program. Individual plant component simulators (i.e., steam generator, reactor core, etc.) were written by different individuals as separate computational "modules." The steam turbines with feedwater heaters were identified as the simulator module requiring the most computational time.

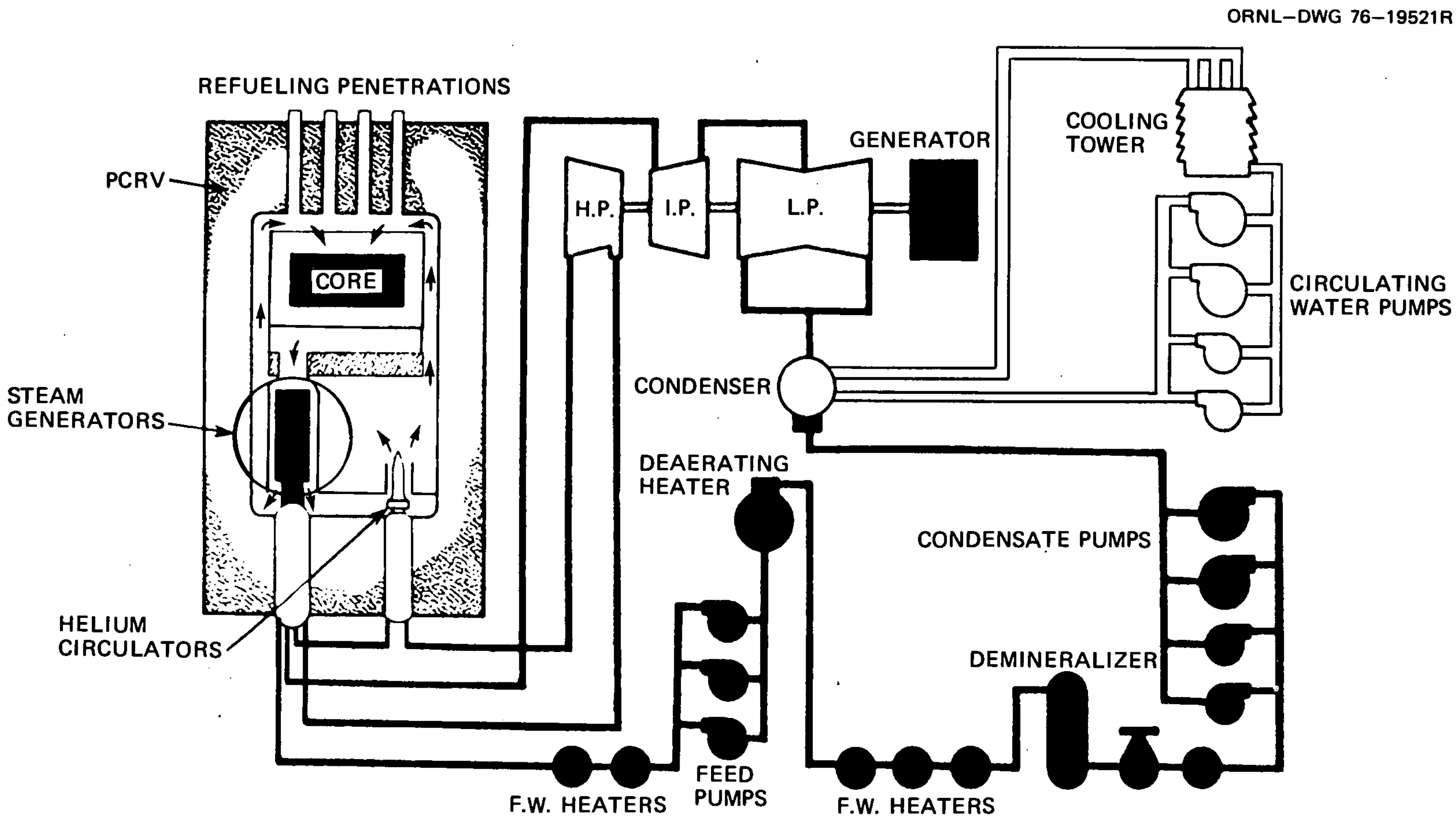

Fig. 1. Flow diagram of the Fort St. Vrain Reactor.

The computer simulation for dynamic behavior of steam turbine components was revised with the objective of maintaining sufficient accuracy while reducing computation time. This present ORTURB simulation uses equations similar to those presented for the steam turbine model[1] but uses a modeling and iteration scheme that reduces computer time by minimizing floating point exponentiation. ORTURB was developed and debugged independently of ORTAP and hence required inclusion of FORTRAN statements in a main driver subroutine to provide the necessary transient input parameters. In ORTAP, these parameters are supplied by appropriate plant component simulations.

The ORTURB program is divided into three main parts: the driver subroutine; turbine subroutines to calculate the pressure-flow balance of the high-, intermediate-, and low-pressure turbines; and feedwater heater subroutines. This feedwater heater model is substantially modified from the original ORTAP feedwater heater model as developed by Delene.[2] Necessary steam property subroutines, obtained from Ref. 3, were also taken from this same report.

The ORTURB program has two important limitations: (1) the turbine shaft is assumed to rotate at a constant (rated) speed of 3600 rpm; and (2) energy and mass storage of steam in the high-, intermediate-, and low-pressure turbines is assumed to be negligible. These limitations, which were also true of the original ORTAP turbine plant model, exclude the use of ORTURB during a turbine transient such as startup from zero power or very low turbine flows. The ORTURB program may be obtained on request from the author.

2. HIGH-PRESSURE TURBINE SIMULATION

The basic governing equation for pressure and flow balance of high-pressure turbines (HPT) is the ideal gas flow law:

$$W = A \left\{ \frac{k}{k-1} \left(\frac{P_1}{\nu_1} \right) \left[\left(\frac{P_2}{P_1} \right)^{\frac{2}{k}} - \left(\frac{P_2}{P_1} \right)^{\frac{k+1}{k}} \right] \right\}^{\frac{1}{2}} , \tag{1}$$

where

k = isentropic exponent,

P = pressure,

ν = specific volume,

A = represents a flow constant, and

W = flow.

The subscript 1 refers to an upstream value, and the subscript 2 refers to a downstream value.

Use of this equation allows the effect of a downstream pressure variation to be reflected upstream when the pressure ratio (downstream to upstream pressure) is greater than critical. This is an important consideration in predicting the transient performance of the high-pressure turbine whose exhaust pressure will be affected by steam turbines driving the four helium circulators (Fig. 2).

The high-pressure turbine has been divided into three stage groups: the governing stage, including the flow control valve, and two reaction stage groups (Fig. 2). It was necessary to use this detail and suffer the computational expense to properly calculate governing-stage shell pressure. This shell pressure is a feed-forward signal for the plant feedwater flow controller and is primarily determined by the flow-passing ability of the following reaction stages.

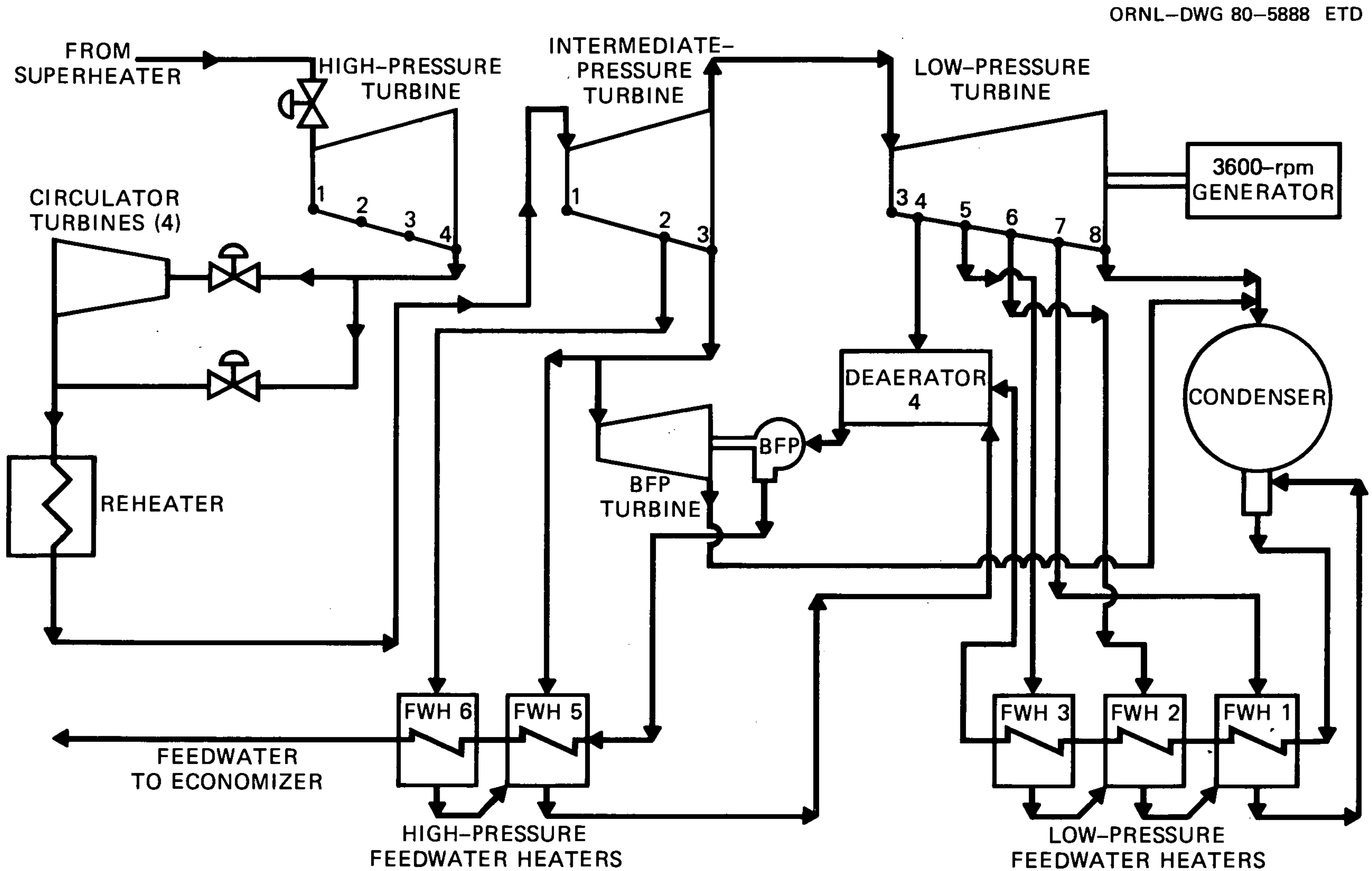

Fig. 2. Fort St. Vrain Reactor turbine-generator plant flow diagram.

Shell pressure of the governing stage at 100% power is determined from initial conditions, assuming that the governing stage is designed according to Chap. 8, article 2 of Ref. 4. The most significant part of this assumption is that the ratio of governing-stage wheel speed to theoretical steam velocity is 0.5 for a one-row wheel at design load.

The ratio of published exit pressure[5] to this determined governing-stage shell pressure was found to be less than the critical pressure ratio. The following reaction stages were then modeled as two stage groups so that the stage-group pressure ratios (P_{exit}/P_{inlet}) of each would be greater than critical. This allows downstream exit pressure variations, which affect the flow-passing ability of the reaction stages, to be reflected upstream to the governing-stage shell pressure.

High-pressure turbine thermal efficiency is calculated from input data at 100% power and corrected for off-normal conditions by the methods presented in Ref. 6. Two important design factors, the governing-stage pitch diameter (762 mm) and the number of rows of moving buckets of the governing stage (1), were obtained by applying the methods and information from Ref. 6 to published heat balances[5] at 100 and 25% power.

High-pressure turbine flow constants are determined from input data at design load conditions and are assumed to be constant throughout the simulation. The flow control valve is simulated by varying the governing-stage flow constant during a calculation to control the flow through the turbine.

After initialization calculations, turbine flows are calculated from pressure distribution. Then, mass flows are checked at stage-group boundary points to ensure that flows are balanced within a specified tolerance. If flows are unbalanced at one point, pressure at that point is appropriately modified, and a resultant mass flow rate is calculated from one stage group upstream to one stage group downstream of the point in question using Eq. (1). Turbine stage-group flows are again checked, and if all are balanced within tolerance, the turbine iterations are completed. If flows are again unbalanced at any point, pressure is changed and the two-stage group flow calculation is again performed. Use of this two-stage group technique, instead of recalculation of the entire turbine, minimizes the floating point exponentiation made necessary by the ideal gas flow equation.

While most minor flows in the turbine were neglected, the packing gland flow from the high-pressure turbine exit to the shell of feedwater heater 5 was not ignored because a relatively large amount of energy is carried by the flow. This flow is determined throughout a transient simulation by assuming that pressure drop from the turbine exhaust to the shell of feedwater heater 5 is due to a shape loss, with the proportionality constant determined from input data at design load. This flow is calculated after high-pressure turbine iterations are complete, and it is subtracted from the exit flow of the high-pressure turbine.

3. REGENERATIVE INTERMEDIATE- AND LOW-PRESSURE TURBINE SIMULATIONS

Assumptions and approximations were also made to simplify the calculation of transient performance of the intermediate- and low-pressure turbines (ILPT).

Figure 2, a schematic of intermediate- and low-pressure turbines, shows steam extraction points from the turbines and connections to the feedwater heaters. Dynamics of crossover piping connecting the intermediate turbine exhaust with the low-pressure turbine inlet are ignored. Volume and mass inventory inside this pipe are quite small compared with the main steam piping or the deaerator, so dynamic response of the crossover piping would be essentially instantaneous as compared with the response of other components. Therefore, the ILPT is considered a single entity.

This analysis assumes that the external conditions experienced by the individual components do not change during a timestep. Each of five feedwater heaters and the deaerator are considered separate components, as are the feed-pump turbine and the ILPT.

The ILPT is divided into seven stage groups separated by points representing the turbine inlet, six steam extraction points, and the condenser. During initialization calculations, the stage-group flow constant for the ideal gas flow equation and the stage-group thermal efficiency are calculated for each stage group. The stage-group flow constant remains unchanged throughout a simulated transient, whereas the stage-group thermal efficiency is corrected for turbine inlet volume flow.[7]

This stage-group thermal efficiency correction is necessary because fixed stage losses, such as root and tip interference losses and rotation losses, have less effect on overall stage-group efficiency as the steam volumetric flow increases. The correction curve should have a hyperbolic shape but has been linearized for simplicity. This assumption is reasonably accurate for high volume flows but would overestimate stage group thermal efficiency at very low flows.

To accurately model ILPT reaction stages, the pressure ratio across each computational grouping of reaction stages should be greater than critical, with the exception of the last stage which (for condensing turbines) has critical flow at design conditions. Perturbations of the flow-passing ability of a stage group because of downstream pressure fluctuations such as feedwater heater transients can be accounted for with the ideal gas flow equation if the pressure ratio is greater than critical. The pressure ratios across stage groups for the design power condition are generally slightly less than critical. This condition means that a downstream pressure increase, such as that caused by stopping extraction flow to a feedwater heater, would have to increase the stage-group pressure ratio above critical before stage-group flow is affected by a downstream pressure rise.

The ILPT modeling could be made more accurate by an increase in the number of computational stage groups and an assurance that the pressure ratio across each group (except for the last) is greater than critical. These changes, however, would entail an increased computation cost due to the increased amount of floating point exponentiation required to represent the ideal gas flow equation. Present ILPT modeling is sufficiently accurate for use in an overall steam plant dynamic simulation, considering the accuracy of existing turbine design data available.

Pressure at an extraction point determines extraction flow to the shell-side of a feedwater heater. Pressure loss in the extraction pipe is assumed to be a shape, or form, loss as expressed by

$$\frac{\Delta P_{ex}}{\rho} = K_{ex} \frac{v^2}{2g_c} \; . \qquad (2)$$

Multiplying both sides by the square of the density, and the right-hand side (RHS) by (A_f^2/A_f^2),

$$\rho\Delta P = \frac{K_{ex}}{A_f^2} \frac{(\rho A_f v)^2}{2g_c} \; , \qquad (3)$$

and the mass flow W_{ex} is

$$W_{ex} = \rho A_f v \; . \qquad (4)$$

Substituting Eq. (4) into Eq. (3), collecting constants, and rearranging:

$$W_{ex} = \sqrt{\frac{\rho \Delta P}{K'_{ex}}} , \tag{5}$$

where

$$K'_{ex} = \frac{\rho i \Delta P i}{W^2_{ex,i}} \tag{6}$$

and i represents initial conditions at the extraction point. Substituting Eq. (6) into Eq. (5)

$$W_{ex} = W_{ex,i} \sqrt{\frac{\rho \Delta P}{\rho_i \Delta P_i}} \tag{7}$$

or

$$W_{ex} = W_{ex,i} \sqrt{\frac{\nu_i}{\nu} \cdot \frac{\Delta p}{\Delta P_i}} . \tag{8}$$

Since steam property subroutines used in ORTURB calculate specific volume rather than density, Eq. (8) is used. Equation (1) can be shown to reduce to Eq. (8) for small pressure drops.

During turbine iterations, if feedheater shell pressure is greater than extraction point pressure, extraction flow is set to zero (no reverse flow) until the extraction pressure is again greater than shell pressure.

The feed-pump system for Fort St. Vrain consists of three pumps, two driven by steam turbines and one by an electric motor. The steam enthalpy drop across the feed-pump turbines is added to the enthalpy of feedwater flowing through the pumps. Energy imparted to the feedwater by electric feed pump is ignored. This, in effect, assumes that feed-pump thermal efficiency is 66.7%. These results agree well with published heat balances.[5] For simplicity, the feed-pump system for the steam-side is modeled as one steam turbine-driven pump. Feedwater flow through the pump is determined by the plant controller simulator and not turbine steam conditions. This simplification could be modified by substituting a feedwater pump computer simulation.

The feed-pump turbine has been modeled as one stage group, meaning that entrance and exit pressures are used as upstream and downstream pressures in the ideal gas flow equation. Inlet pressure is set equal to pressure at the second ILPT extraction point (point 3 of Fig. 2), and exit pressure is set equal to main condenser pressure. No flow control device is modeled for the feed-pump turbine, which means that the flow is dependent on inlet steam conditions and outlet steam pressure if flow is less than critical. A steam-flow control device could easily be added if necessary.

Turbine flows resulting from the previous-time pressure distribution are all calculated initially for a timestep. The turbine flow upstream from an extraction point is then compared with the turbine flow downstream and the extraction flow. If the flows do not balance, extraction pressure is modified accordingly, and the two-stage group flow calculation is repeated (as described for the HPT) until convergence is obtained. Test cases were run in which the entire turbine flow distribution was recalculated when only one pressure changed during the iteration process. No significant differences in converged flows from the two-point case were noticed, but computer time was greatly increased.

Low-pressure turbine exhaust loss is calculated according to the procedure in Ref. 6. This loss is a unique function of steam velocity at the discharge of the last-stage bucket. Empirical data are used for this procedure and were developed from known dimensions (851-mm active length on the last-stage bucket) and published exhaust losses[5] at 100 and 25% power.

As the pressure-flow iteration advances through the turbine, required steam properties of temperature and specific volume are obtained from steam property subroutines originally written for the ORCENT code[3] rather than the ASME 1967 steam table equations.[8] The ORCENT subroutines have fewer iterative loops, thus consuming less computer time than ASME equations, and are of sufficient accuracy for transient analysis of steam turbines.

4. FEEDWATER HEATER SIMULATION

The feedwater heater model used in the simulator is shown in Fig. 3. There are five such feedheaters in the simulated turbine plant, located as shown in Figs. 1 and 2.

Steam from the turbines enters the shell of the feedwater heater. If this steam is superheated, the assumption is that it will first lose this superheat to the feedwater by means of a simple heat balance. If the steam is wet, it is divided into a saturated steam part and a saturated liquid part. The liquid falls into a liquid stream on a tray or partition within the feedwater heater. Liquid from a previous feedwater heater may also enter this stream. Because its temperature is usually hotter than the saturated vapor temperature, part of it flashes; this vapor goes into the vapor space. Steam in the vapor space condenses on the tubes containing the feedwater and falls into the liquid stream. This liquid eventually flows into the drain-cooler section of the feedwater heater and loses additional heat to the feedwater as it flows through the drain cooler.

ORNL–DWG 72–12011

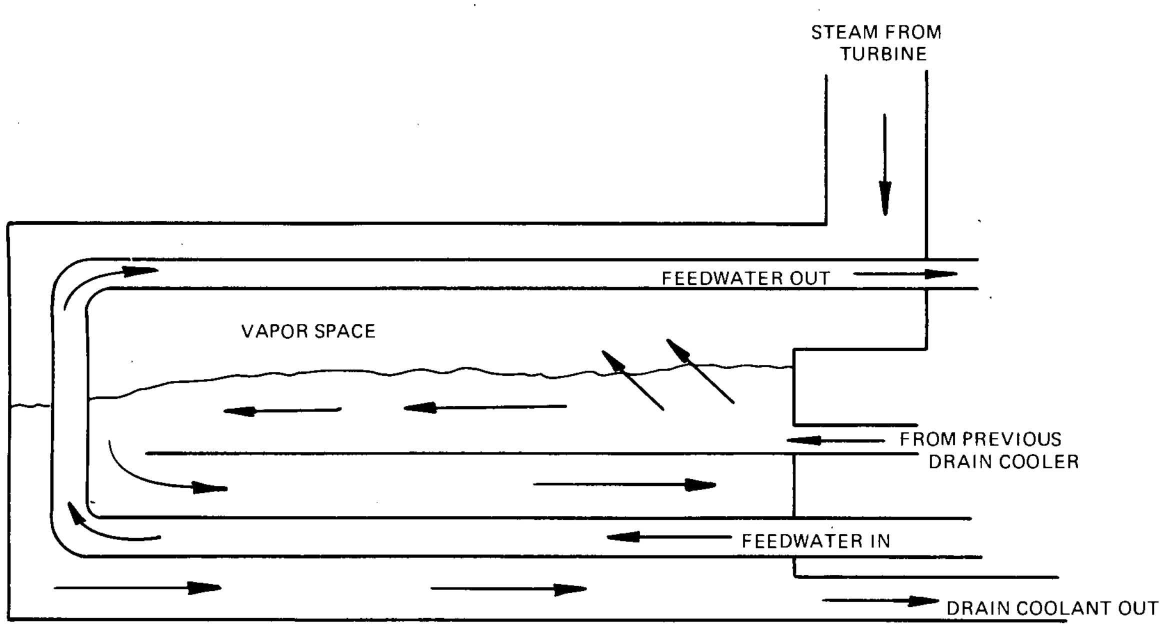

Fig. 3. Feedwater heater.

Feedwater enters the feedwater heater tube bundles and flows counter to the direction of the drain coolant flow. After leaving the drain cooler, feedwater enters tube bundles in the vapor space where it gains additional heat as steam is condensed. Before leaving the heater, feedwater in the tube bundle passes through a superheat section where any superheat in the turbine extraction steam is removed.

In the simulation, the drain-cooler section of the feedwater heater is treated as a counterflow heat exchanger. The feedwater heater section in which feedwater tubes pass through the vapor space is treated as a tube-in-shell heat exchanger with a uniform shell-side temperature. The superheat section heat balance is

$$W_{s,i}\ h_{SH} = W_{FW}\ \Delta h_{FW}\ . \tag{9}$$

The steam flowing into the feedwater heater shell divides into two streams,

$$W_s = W_v + W_\ell\ , \tag{10}$$

such that

$$W_s h_s = W_v h_v + W_\ell h_\ell\ . \tag{11}$$

The liquid entering from a previous drain cooler divides into two streams,

$$W_{DC,i} = W_{DC,f} + W_{DC,\ell}\ , \tag{12}$$

such that

$$W_{DC,i}\ h_{DC,i} = W_{DC,f}\ h_{fg} + W_{DC,\ell}\ h_{DC,\ell}\ , \tag{13}$$

where h_{fg} and $h_{DC,\ell}$ are evaluated at the vapor temperature T_v.

The vapor condensing rate W_c is calculated by

$$W_c = \frac{(UA)_{EV}}{h_{fg}}\ (T_v - T_{FE,\phi}) + \frac{(UA)_{EV}}{h_{fg}}\ (T_v - T_{FE,A})\ . \tag{14}$$

$(UA)_{EV}$ is the heat transfer coefficient multiplied by the area over one-half the evaporator length. $(UA)_{DC}$ is the heat transfer coefficient multiplied by the area over one-half the drain-cooler length. These coefficients are assumed to be constant in the simulation.

A lumped parameter model was constructed using seven differential equations to describe the dynamics of a single feedwater heater unit (Fig. 4). All seven differential equations are for temperature.

Feedwater temperatures in the drain cooler section are represented by Eqs. (15) and (16), which were derived from a time-dependent energy balance:

$$\frac{dT_{FC,\phi}}{dt} = \frac{2W_{FW}}{M_{FC}} (T_{FC,A} - T_{FC,\phi}) + \frac{2(UA)_{DC}}{(MC_p)_{FC}} (T_{DC,A} - T_{FC,\phi}) , \tag{15}$$

$$\frac{dT_{FC,A}}{dt} = \frac{2W_{FW}}{M_{FC}} (T_{FW,i} - T_{FC,A}) + \frac{2(UA)_{DC}}{(MC_p)_{FC}} (T_{DC,\phi} - T_{FC,A}) . \tag{16}$$

Equations (17) and (18) represent feedwater temperatures in the evaporator, or vapor section:

$$\frac{dT_{FE,\phi}}{dt} = \frac{2W_{FW}}{M_{FE}} (T_{FE,A} - T_{FE,\phi}) + \frac{2(UA)_{EV}}{(MC_p)_{FE}} (T_v - T_{FE,\phi}) , \tag{17}$$

$$\frac{dT_{FE,A}}{dt} = \frac{2W_{FW}}{M_{FE}} (T_{FC,\phi} - T_{FE,A}) + \frac{2(UA)_{EV}}{(MC_p)_{FE}} (T_v - T_{FE,A}) . \tag{18}$$

Temperature of the coolant in the drain cooler is represented by Eqs. (19) and (20):

$$\frac{dT_{DC,\phi}}{dt} = \frac{2W_{DC}}{M_{DC}} (T_{DC,A} - T_{DC,\phi}) + \frac{2(UA)_{DC}}{(MC_p)_{DC}} (T_{FC,A} - T_{DC,\phi}) , \tag{19}$$

$$\frac{dT_{DC,A}}{dt} = \frac{2W_{DC}}{M_{DC}} (T_\ell - T_{DC,A}) + \frac{2(UA)_{DC}}{(MC_p)_{DC}} (T_{FC,\phi} - T_{DC,A}) . \tag{20}$$

The seventh differential equation for T_v, the saturation temperature of vapor in the feedwater heater shell, depends on mass flow rate into and

ORNL–DWG 72–12012R

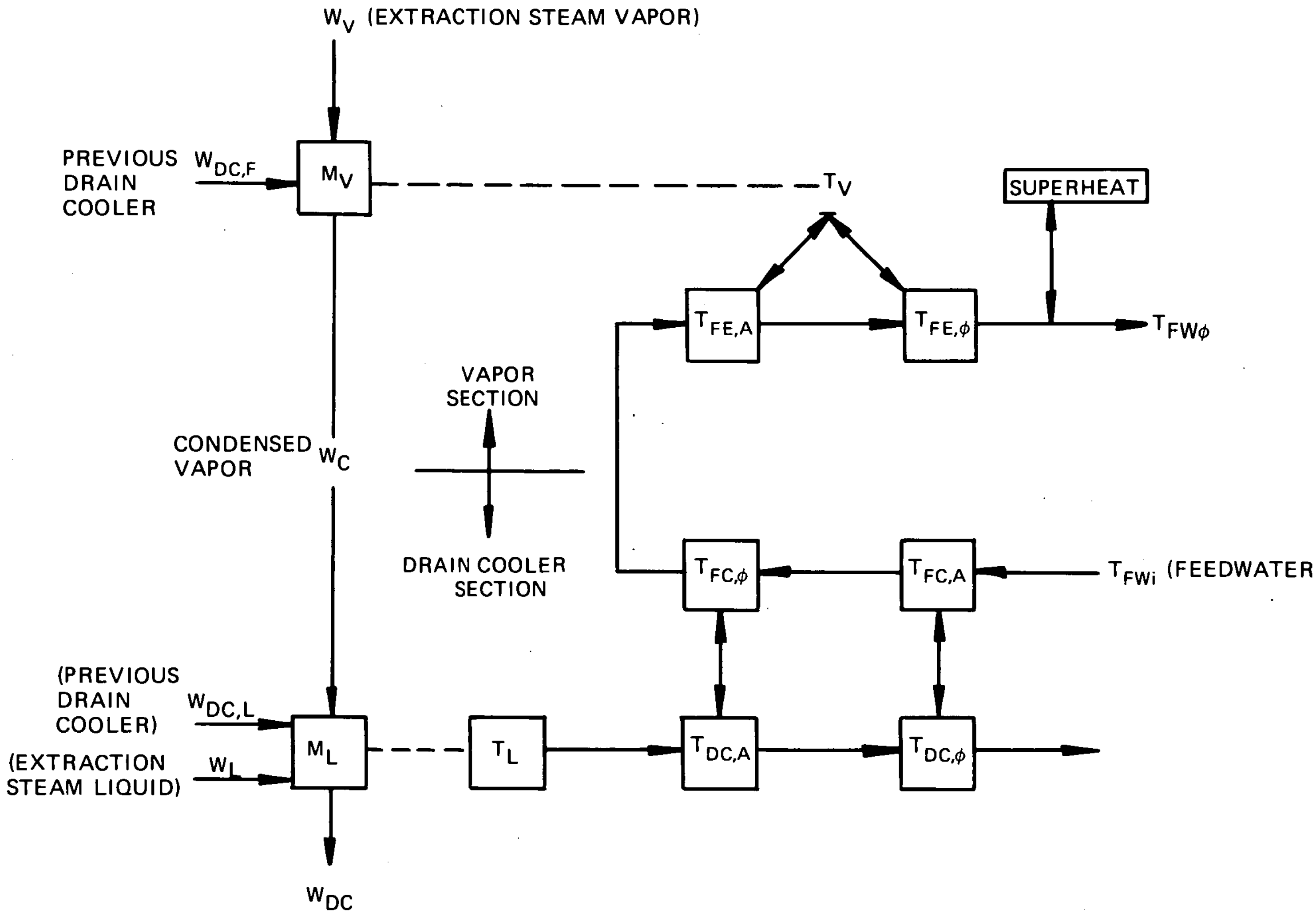

Fig. 4. Flow diagram of simulated feedwater heater.

out of the shell in the following manner:

$$\frac{dT_v}{dt} = \left.\frac{dT}{dP}\right|_{sat} \cdot \frac{dP}{dt} = \left.\frac{dT}{dP}\right|_{sat} \cdot \left.\frac{dP}{d\rho}\right|_{sat} \cdot \frac{1}{V} \cdot \frac{dM}{dt} . \tag{21}$$

The shell vapor mass rate of change dM/dt is the net flow into the feedheater shell,

$$\frac{dM}{dt} = W_v + W_{DC,f} - W_c . \tag{22}$$

Combining Eqs. (22) and (14) with Eq. (21), the seventh differential equation is

$$\frac{dT_v}{dt} = \left[\left.\frac{dT}{dP}\right|_{sat} \cdot \left.\frac{dP}{d\rho}\right|_{sat} \cdot \frac{1}{V}\right]$$

$$\times \left\{W_v + W_{DC,f} - \left[\frac{(UA)_{EV}}{h_{fg}}\right] \cdot (2 \cdot T_v - T_{FE,A} - T_{FE,\phi})\right\} . \tag{23}$$

Saturation derivatives are reevaluated at the beginning of each timestep using the previous timestep value of pressure and density. Shell pressure is determined from the saturation temperature, T_v.

The value T_ℓ in Eq. (20), representing the temperature of the liquid going from the shell to the drain cooler, is obtained from an energy balance of shell liquid flow and enthalpy with condensation flow and energy using the previous timestep values. Since flashing of this shell liquid back to steam is not represented, the value of T_ℓ should be monitored during a simulated transient to ensure that it does not rise significantly above the saturation temperature T_v.

Flow from the drain cooler W_{DC} is assumed to be constant during a timestep and is calculated at the beginning of each timestep by

$$W_{DC} = W_{DC,\ell} + W_\ell + W_C . \tag{24}$$

The set of seven differential equations (15–20, 23) are solved each timestep using the matrix exponential method,[9] as discussed in Ref. 10.

In initializing steady-state calculation, the various masses (M_{DC}, M_{FC}, M_{FE}) are calculated, using a holdup time supplied as an input. During a transient, these masses are corrected for changes in saturated water density caused by temperature changes from initial conditions. Temperature input data include inlet and outlet feedwater temperatures ($T_{FW,i}$ and $T_{FW,\phi}$) and drain cooler inlet and outlet temperatures ($T_{DC,i}$ and $T_{DC,\phi}$). The saturated vapor temperature T_v is determined from input shell vapor pressure. Flow rate input data include steam flow rate W_s, feedwater flow rate (W_{FW}), and the drain cooler flow rates W_{DC} and $W_{DC,i}$. From this data, two of the seven state variables for each feedwater heater ($T_{FE,\phi}$ and $T_{DC,\phi}$) are known. The temperature of feedwater leaving the drain cooler region $T_{FC,\phi}$ may be calculated from the following heat balance:

$$W_{FW} \ (h_{FC,\phi} - h_{FW,i}) = W_{DC} \ (h_{\ell} - h_{DC,\phi}) \ . \qquad (25)$$

The feedwater temperature halfway through the evaporator, $T_{FE,A}$ is determined as shown on the following schematic.

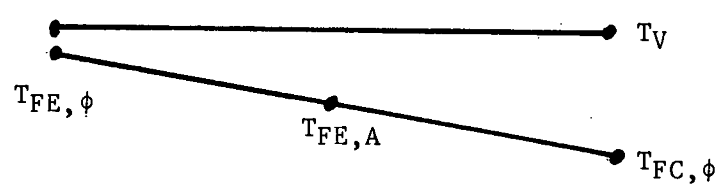

From a heat balance,

$$W_{FW} \cdot C_p(T_{FE,\phi} - T_{FC,\phi}) = 2(UA)_{EV} \ \Delta T_{\ell m} \ , \qquad (26)$$

where $\Delta T_{\ell m}$ is the log mean temperature difference:

$$\Delta T_{\ell m} = \left[(T_v - T_{FC,\phi}) - (T_v - T_{FE,\phi})\right] \Big/ \ell n \frac{T_v - T_{FC,\phi}}{T_v - T_{FE,\phi}} \ . \qquad (27)$$

Substituting Eq. (27) into Eq. (26) and rearranging,

$$\frac{(UA)_{EV}}{W_{FW}C_p} = \frac{1}{2} \ \ell n \ \frac{T_v - T_{FC,\phi}}{T_v - T_{FE,\phi}} \ . \qquad (28)$$

Analogous reasoning will yield the following expression for $T_{FE,A}$:

$$T_{FE,A} = T_V - (T_V - T_{FC,\phi})\exp\left[-\frac{(UA)_{EV}}{W_{FW}C_p}\right] , \tag{29}$$

where all terms on the RHS are known.

In the drain-cooler section, $T_{FC,A}$ and $T_{DC,A}$ are chosen as the temperatures halfway along the feedwater coolant pipe and the drain cooler, respectively. Following the analysis presented by Giedt,[11] which is the classic NTU (number of transfer units) analysis for heat exchangers, these temperatures are obtained by solving two simultaneous equations,

$$T_{DC,A} = T_{DC,i} - E_h(T_{DC,i} - T_{FC,A}) , \tag{30}$$

$$T_{DC,\phi} = T_{DC,A} - E_h(T_{DC,A} - T_{FW,i}) , \tag{31}$$

where the heat exchanger heating effectiveness E_h is

$$E_h = 1 - \exp\left(-\left\{\frac{(UA)_{DC}}{(WC_p)_{DC}}\left[1 - \frac{(WC_p)_{DC}}{(WC_p)_{FW}}\right]\right\}\right)\Bigg/1 - \frac{(WC_p)_{DC}}{(WC_p)_{FW}}\exp\left(-\left\{\frac{(UA)_{DC}}{(WC_p)_{DC}}\left[1 - \frac{(WC_p)_{DC}}{(WC_p)_{FW}}\right]\right\}\right) . \tag{32}$$

The deaerator (feedwater heater 4) is treated as a large mixing tank. Mass and enthalpy inventory calculations are performed at each timestep and resulting equations are solved by Euler's method. The resulting homogenous liquid is assumed to be at saturated conditions.

5. CONTROL

As ORTURB is intended to be used as a part of an overall Fort St. Vrain plant simulator code (ORTAP), certain parameters must be supplied to ORTURB to execute it independently. These time-dependent parameters are desired turbine loading, high-pressure turbine inlet steam pressure and enthalpy, intermediate turbine inlet pressure and enthalpy, and feedwater flow through each feedheater and into the steam generator. These parameters are supplied by the appropriate ORTAP simulator to the version of ORTURB presently implemented in ORTAP. However, to execute ORTURB by itself, these parameters are written into coding of its main program. Coding modifications to the main driver subroutine must be made to represent any other transient.

Feedwater flows of the tube-side of heaters 5 and 6 and the outlet flow of the deaerator are set to the desired steam generator flow rate. Feedwater flow of the tube-side of feedheaters 1 through 3 is set so that the deaerator has a constant fluid level. No attempt is made to balance flow in the condenser.

The drain coolant flows (shell-side only) from feedheaters 1, 2, 3, 5, and 6 are controlled so that the flow into the drain cooler equals the flow out (i.e., constant liquid level).

6. RESULTS

A simulated turbine runback from 100 to 25% electrical power achieved very good agreement in steady state with the 25% power heat balance[5] (Appendix B and Fig. 5). The values in parentheses in Fig. 5 are calculated results from ORTURB. A small portion of the information presented in the 25% power heat balance was used during turbine initialization (low-pressure turbine leaving loss and high-pressure turbine exit steam conditions needed to calculate thermal efficiencies). However, all turbine flows, enthalpies, and pressures were in very good agreement with the heat balance at 25% power (Fig. 5) when initialization was done with the information representing 100% power (Fig. 6).

Transients representing loss-of-condenser, loss-of-feedwater heater, and high-pressure turbine exit pressure fluctuations were also simulated. The turbine model indicated appropriate responses for all simulated transients. Comparisons with actual plant data can easily be made when the information becomes available.

During the modeling for the loss-of-condenser transient, convergence difficulties were noted for the ILPT segments close to the condenser. The subroutine ZER01, a slightly modified version of the subroutine ZEROIN,[12] was then used to bring the pressure-flow distribution into convergence. The mass flow convergence tolerance also required modification during simulation of this severe transient.

The ORTURB turbine model uses approximately 0.05 s of IBM Model 360/91 computer time for each computational timestep. This value is subject to the transient being modeled and will increase as the severity of the transient increases. However, this reduced computer time is a significant improvement as compared to the earlier turbine model in ORTAP.[1]

ORNL–DWG 80–6011 ETD

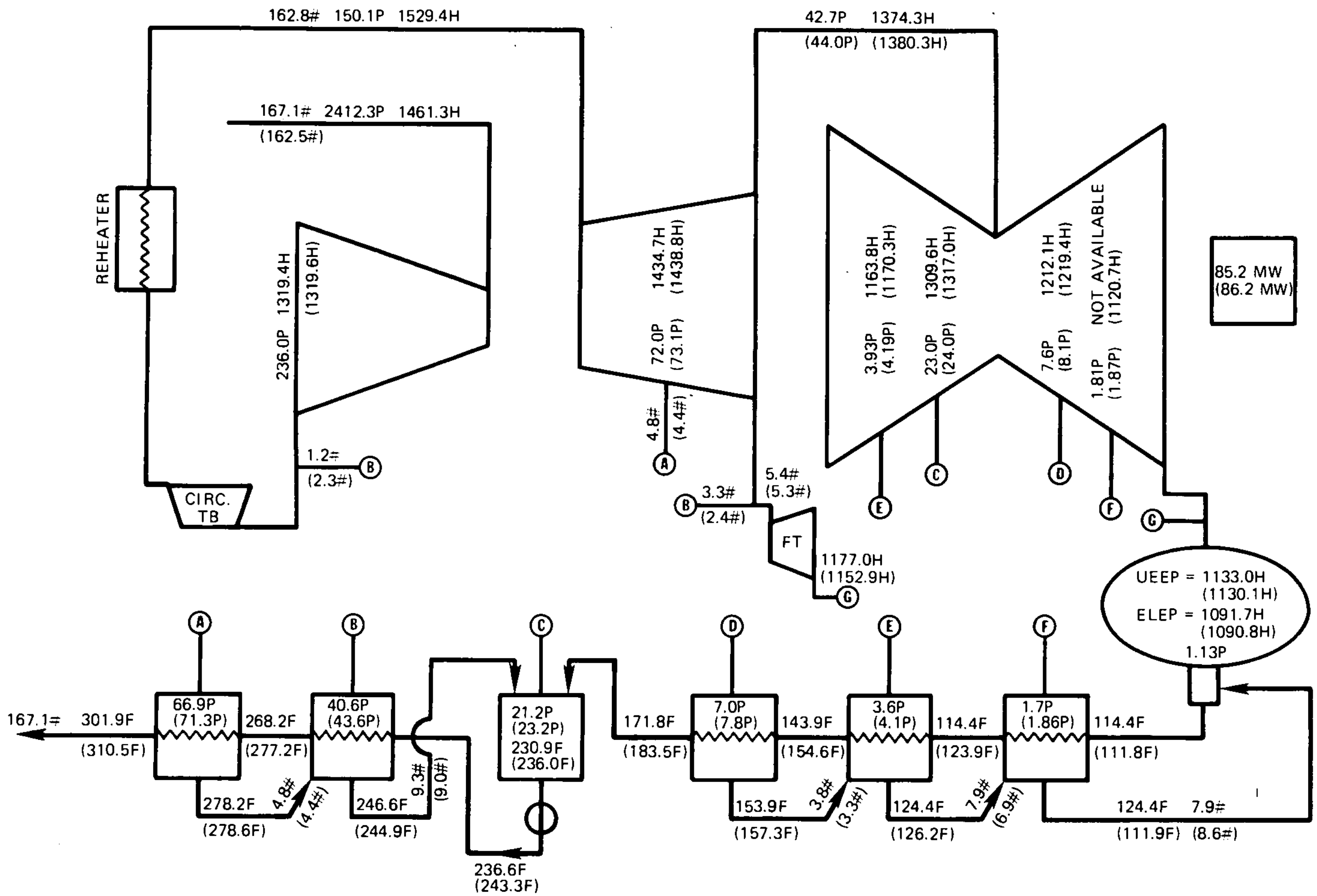

= FLOW (lb_m/s) P = PRESSURE (psia) H = ENTHALPY (Btu/lb_m) F = TEMPERATURE (^{o}F)

ORTURB CALCULATED RESULTS ARE IN PARENTHESES

Fig. 5. Turbine conditions at 25% power heat balance.

ORNL–DWG 80–6012 ETD

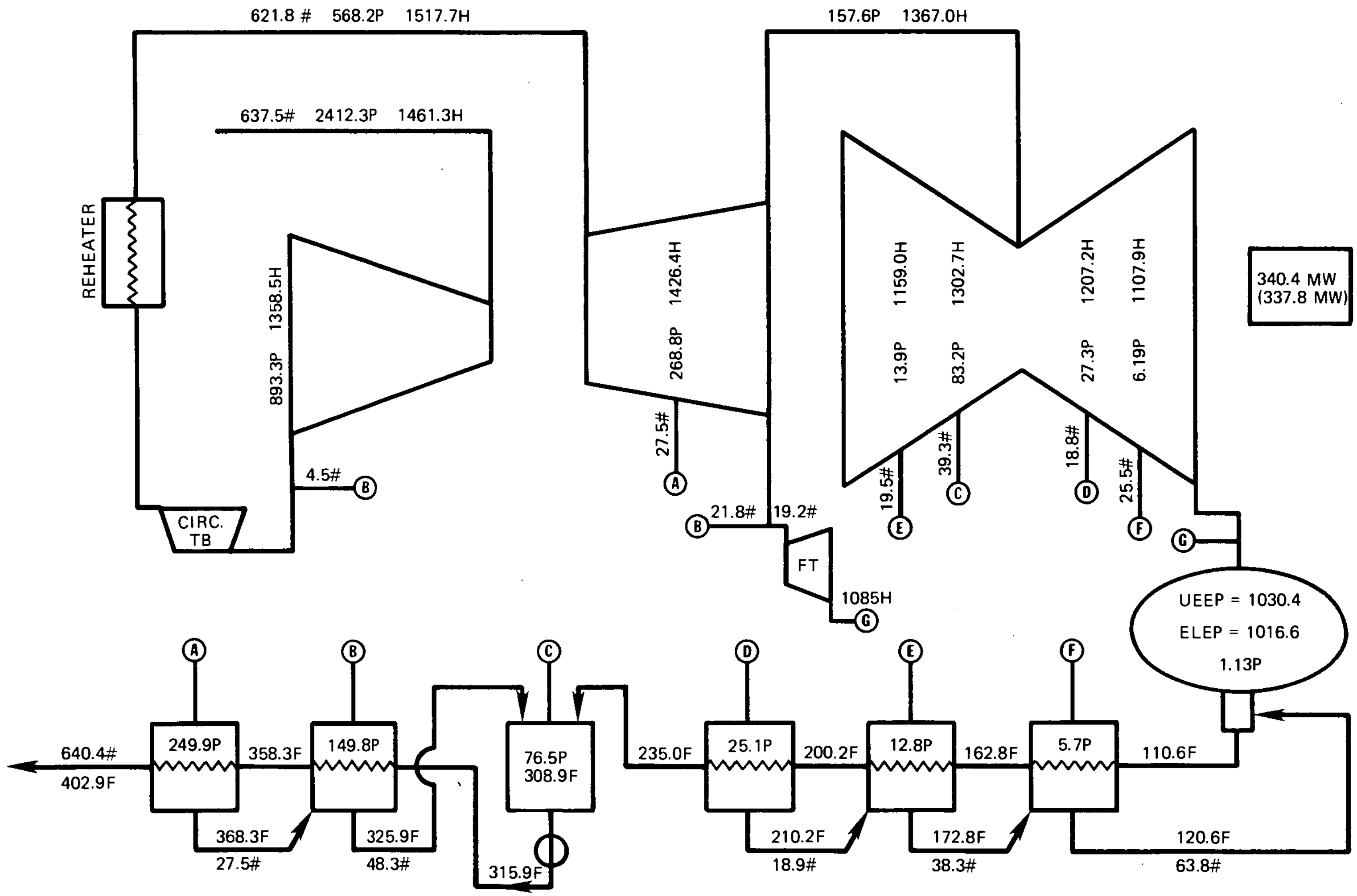

= FLOW (lb_m/s) P = PRESSURE (psia) H = ENTHALPY (Btu/lb_m) F = TEMPERATURE (^oF)

Fig. 6. Turbine initial conditions at 100% power heat balance.

REFERENCES

1. J. C. Cleveland et al., *ORTAP: A Nuclear Steam Supply System Simulation for the Dynamic Analysis of High-Temperature Gas-Cooled Reactor Transients,* ORNL/NUREG/TM-78 (September 1977).

2. J. G. Delene, *A Digital Computer Code for Simulating the Dynamics of Demonstration Size Dual-Purpose Desalting Plants Using a Pressurized Water Reactor as a Heat Source,* ORNL/TM-4104 (September 1973).

3. H. I. Bowers, *ORCENT: A Digital Computer Program for Saturated and Low Superheat Steam Turbine Cycle Analysis,* ORNL/TM-2395 (January 1969).

4. J. K. Salisbury, *Steam Turbines and Their Cycles*, Robert E. Krieger Publishing Co., Huntington, New York, 1974.

5. F. E. Swart, Public Service Company of Colorado, letter to J. C. Conklin, Oak Ridge National Laboratory, Feb. 8, 1977.

6. R. C. Spencer, K. C. Cotton, and C. N. Cannon, *A Method for Predicting the Performance of Steam Turbine Generators...16,500 kW and Larger*, General Electric Co., GER-2007C (July 1974).

7. H. Hegetschweiler and R. L. Bartlett, "Predicting Performance of Large Steam Turbine-Generator Units for Central Stations," *Trans. ASME* 79, 1086 (1957).

8. C. A. Meyer, R. B. McClintock, G. J. Silvester, and R. C. Spencer, *Thermodynamic and Transport Properties of Steam,* Am. Soc. of Mech. Eng., New York (1967).

9. S. J. Ball and R. K. Adams, *MATEXP, A General Purpose Digital Computer Program for Solving Ordinary Differential Equations by the Matrix Exponential Method*, ORNL/TM-1933 (August 1967).

10. J. G. Delene and S. J. Ball, *A Digital Computer Code for Simulating Large Multistage Flash Evaporator Desalting Plant Dynamics,* ORNL/TM-2933 (September 1971).

11. W. H. Giedt, *Principles of Engineering Heat Transfer,* D. Van Nostrand Co., Inc., Princeton, N.J. (January 1957).

12. G. F. Forsythe, M. A. Malcolm, and C. B. Moler, *Computer Methods for Mathematical Computations*, Prentice-Hall, Englewood Cliffs, N.J. (1977).

Appendix A

INPUT REQUIREMENTS

Refer to Figs. 2 and 6.

Cards No. 1 (FORMAT 20A4)

Two title cards

Card No. 2 (FORMAT I5)

NOSGS — number of steam generator modules feeding the high-pressure turbine (for FSV set equal to 12).

Card No. 3 (FORMAT 2E10.3, I10)

TSTRT — starting time

DT — time step

NTMSP — desired number of time steps

Card No. 4 (FORMAT 2E10.3)

P — desired precision of the A-matrix for feedwater heater calculations. Experience with different values of this parameter will be necessary to evaluate the trade-offs of computational accuracy and computer time (recommend 10^{-6} for IBM computers).

ATOL — desired fractional change of each of the seven calculated state variables of the feedwater heater calculation before updating the A-matrix. Again, experience is necessary to evaluate the trade-offs of computer accuracy and time (recommend 0.01).

Card No. 5 (16I5)

IND(I), I=1 through 16 set to zero except the following.

IND(3) — desired number of time steps between printouts.

IND(4) — set not equal to zero if A-matrix information is desired output wherever updated (for debugging).

IND(5) — set not equal to zero if the forcing function vector is desired during printouts (for debugging).

Card No. 6 (2E10.3)

ABSTOL — absolute tolerance (lbm)

RELTOL — relative tolerance (fraction)

The actual tolerance used by ORTURB during the pressure-flow iterations for both the HPT and ILPT is of the form:

$$TOL = ASBTOL + W_{upstream} \cdot RELTOL$$

Card No. 7 (6E10.3)

WHP100 — inlet flow to high-pressure turbine (HTP) at 100% power (lbm/s).

PHPT0 — inlet pressure to HPT at 100% power (psia)

PHPEX0 — exhaust pressure from HPT at 100% power (psia)

HHP100 — inlet enthalpy to HPT at 100% power (Btu/lbm)

HHPEX0 — exhaust enthalpy from HPT at 100% power (Btu/lbm)

WHPLK0 — packing-gland leak flow rate from HPT exhaust to the shell of feedwater heater 5 (lbm/s)

Card No. 8 (FORMAT E10.3)

HCON — condenser outlet enthalpy (Btu/lbm)

Card No. 9 (FORMAT 7E10.3)

WILP(I), I=1 through 7 — 100% power mass flow in each of the intermediate- and low-pressure turbine (ILPT) segments (lbm/s)

Card No. 10 (FORMAT 8E10.3)

PILP(I), I=1 through 8 — 100% power pressure at the beginning of the ILPT segments (psia)

Card No. 11 (FORMAT 8E10.3)

HILP(I), I=1 through 8 — 100% power enthalpy at the beginning of the ILPT segments (Btu/lbm)

Card No. 12 (FORMAT 5E10.3)

PFPTI0 — pressure at inlet to feedpump turbine (FT) at 100% power (psia)

HFPTI0 — enthalpy at inlet to FT at 100% power (Btu/lbm)

PFPT0 — exhaust pressure of FT at 100% power (psia)

HFPT0 — exhaust enthalpy of FT at 100% power (Btu/lbm)

WFPT0 — flow of FT at 100% power (lbm/s)

Card No. 13 (FORMAT 6E10.3)

One card is required for each feedwater heater as numbered on Fig. 2 at 100% power. The deaerator is considered feedwater heater 4.

WDC — drain coolant flow (lbm/s)

WFW — feedwater flow (lbm/s)

TFWI — temperature of feedwater entering heater (°F)

TFWO — temperature of feedwater leaving heater (°F)

TDCO — temperature of liquid leaving drain cooler (°F)

PFHV — vapor pressure in feedheater shell (psia)

Card No. 14 (FORMAT 4E10.3)

One card is required for each feedwater heater at 100% power.

HFWC — holdup time of feedwater in drain-cooler portion (s)

HDC — drain cooler holdup time (s)

HFWE — holdup time of feedwater in evaporator portion (s)

HVFH — steam holdup time on shell-side of feedwater heater (s)

Appendix B

OUTPUT

Output from ORTURB is presented in Fig. B.1 for 100% power conditions and in Fig. B.2 for 25% power conditions. An explanation of the information that is not self-evident follows.

Desired load is a variable that must be specified in the driver routine to control electrical output of the turbine. Actual load is the fraction of 100% power calculated by ORTURB. VLVH is that fraction of

TIME (SEC) = .0

HIGH PRESSURE TURBINE OUTPUT (MWE) = 69.138
LOW PRESSURE TURBINE ELECTRICAL OUTPUT (MWE) = 274.65
TOTAL GROSS ELECTRICAL OUTPUT (MWE) = 337.74
DESIRED LOAD = 1.0000 ACTUAL LOAD = 1.0000 VLVH = 1.0000

HIGH PRESSURE TURBINE EFFICIENCY .808051

HIGH PRESSURE TURBINE DATA

POINT	FLOW	TEMPERATURE	ENTHALPY	PRESSURE
1	637.46	1000.01	1461.30	2412.30
2	636.01	970.66	1449.74	2179.28
3	636.02	874.58	1411.69	1536.29
4	633.08	740.93	1358.50	893.30

INTERMEDIATE AND LOW PRESSURE TURBINE DATA

POINT	FLOW	TEMPERATURE	ENTHALPY	PRESSURE
1	621.87	1000.09	1517.70	568.20
2	594.39	808.58	1426.40	268.80
3	554.16	681.64	1367.00	157.60
4	514.95	544.24	1302.70	83.20
5	496.11	335.43	1207.20	27.30
6	476.64	228.87	1159.00	13.90
7	451.11	171.41	1107.90	6.19
8	470.34	105.83	1029.97	1.13

EXHAUST LOSS (BTU/LBM) = 13.3724

FEEDPUMP FLOW (LBM/S) = 19.230 FEEDPUMP OUTLET ENTHALPY (BTU/LBM) = 1087.1

FEEDHEATER STATE VARIABLES

STG	TFCO	TFCA	TFEO	TFEA	TDCO	TDCA	TFHV
1	115.935	112.396	162.800	151.671	120.600	135.060	167.833
2	165.133	163.720	200.204	191.101	172.800	183.612	205.119
3	201.521	200.840	233.567	224.145	210.200	220.385	240.290
4	0.0	0.0	0.0	0.0	308.980	0.0	0.0
5	318.319	316.696	352.039	342.475	326.000	336.803	358.308
6	360.270	359.322	394.204	384.401	368.300	378.884	400.912

STG	TFWO	TDCO	TFWI	TFHI	WFHC	WDVI	WFHV	WFHL	WDLI	WFW	WDC	TFEI
1	162.800	120.600	110.600	167.833	28.171	0.191	24.885	0.650	38.109	600.890	63.800	115.935
2	200.200	172.800	162.800	205.119	21.639	0.099	19.465	0.0	18.771	600.890	38.300	165.133
3	235.000	210.200	200.200	240.290	20.336	0.0	18.840	0.0	0.0	600.890	18.870	201.521
4	308.980	308.980	235.000	309.041	0.0	0.0	0.0	0.0	0.0	640.360	640.360	235.172
5	358.300	326.000	315.900	358.308	25.940	0.339	24.875	0.0	27.211	640.360	48.250	318.319
6	402.900	368.300	358.900	400.912	28.058	0.0	27.485	0.0	0.0	640.360	27.550	360.270

STG	HFWI	HFEI	HFEO	HFWO	HDCI	HDCO	HFHV	HFHS	WFHS	PFHV
1	78.549	83.560	130.690	130.690	135.728	88.529	1133.307	1107.900	25.535	5.700
2	130.690	132.758	167.829	168.191	173.138	140.701	1147.820	1159.000	19.465	12.800
3	168.191	169.146	201.817	203.277	208.631	178.251	1160.623	1207.200	18.840	25.100
4	203.277	0.0	0.0	278.605	296.507	278.605	1182.249	1302.700	39.396	76.537
5	286.016	288.569	323.664	330.382	330.390	296.507	1194.069	1365.505	24.875	149.800
6	331.016	332.520	368.454	378.125	375.975	341.023	1201.081	1426.400	27.485	249.900

Fig. B.1. ORTURB output printing for initial conditions at 100% power.

TIME (SEC) = 200.00

HIGH PRESSURE TURBINE OUTPUT (MWE) = 24.294
LOW PRESSURE TURBINE ELECTRICAL OUTPUT (MWE) = 64.138
TOTAL GROSS ELECTRICAL OUTPUT (MWE) = 86.215
DESIRED LOAD = 0.2500 ACTUAL LOAD = 0.2553 VLVH = 0.1590

HIGH PRESSURE TURBINE EFFICIENCY .545972

HIGH PRESSURE TURBINE DATA

POINT	FLOW	TEMPERATURE	ENTHALPY	PRESSURE
1	162.48	1000.01	1461.30	2412.30
2	163.39	709.04	1360.55	526.36
3	163.48	654.23	1339.11	376.31
4	160.25	600.18	1319.58	236.00

INTERMEDIATE AND LOW PRESSURE TURBINE DATA

POINT	FLOW	TEMPERATURE	ENTHALPY	PRESSURE
1	162.69	1000.02	1529.40	150.10
2	159.27	817.55	1438.76	73.09
3	152.66	696.86	1380.26	43.98
4	146.44	564.22	1316.97	24.03
5	144.33	353.98	1219.37	8.07
6	141.07	246.07	1170.34	4.19
7	139.19	135.62	1120.70	1.87
8	144.49	105.83	1130.09	1.13

EXHAUST LOSS (BTU/LBM) = 39.2681

FEEDPUMP FLOW (LBM/S) = 5.2975 FEEDPUMP OUTLET ENTHALPY (BTU/LBM) = 1152.9

FEEDHEATER STATE VARIABLES

STG	TFCO	TFCA	TFEO	TFEA	TDCO	TDCA	TFHV
1	112.413	111.839	123.548	122.511	111.933	113.229	123.552
2	127.765	125.027	153.300	150.587	126.171	131.654	153.560
3	158.480	155.855	181.438	178.442	157.265	162.494	181.893
4	0.0	0.0	0.0	0.0	236.073	0.0	0.0
5	246.124	243.914	271.937	268.700	244.913	250.002	272.463
6	279.839	277.702	303.673	300.632	278.555	283.221	304.144

STG	TFWO	TDCO	TFWI	TFHI	WFHC	WDVI	WFHV	WFHL	WDLI	WFW	WDC	TFEI
1	123.890	111.933	111.775	124.233	1.771	0.016	1.177	0.0	6.820	150.970	8.591	112.413
2	154.568	126.171	123.890	154.120	3.568	0.012	3.544	0.0	3.312	150.970	6.880	127.765
3	183.507	157.265	154.568	182.502	3.334	0.0	3.330	0.0	0.0	150.970	3.334	158.480
4	236.073	236.073	183.507	309.041	0.0	0.0	0.0	0.0	0.0	167.100	167.100	235.172
5	277.174	244.913	243.195	272.993	4.668	0.029	4.640	0.0	4.324	167.100	8.992	246.124
6	310.478	278.555	277.174	305.123	4.366	0.0	4.361	0.0	0.0	167.100	4.366	279.839

STG	HFWI	HFEI	HFEO	HFWO	HDCI	HDCO	HFHV	HFHS	WFHS	PFHV
1	79.400	80.359	91.471	91.515	92.155	79.879	1115.231	1120.701	1.582	1.867
2	91.813	95.681	121.189	122.193	122.009	94.089	1127.556	1170.342	3.565	4.058
3	122.457	126.369	149.357	151.132	150.425	125.154	1138.881	1219.374	3.340	7.832
4	151.432	0.0	0.0	204.323	213.336	204.323	1195.254	1316.971	7.139	23.251
5	211.574	214.544	240.807	245.799	241.886	213.316	1171.381	1351.194	4.647	43.584
6	246.159	248.885	273.373	280.103	274.869	247.571	1180.892	1438.760	4.373	71.286

Fig. B.2. ORTURB output printing for initial conditions at 25% power.

the flow constant of the HPT governing-stage necessary to achieve the actual load.

Points 1 through 4 of the high-pressure turbine data are shown on Fig. B.2. Differences in flow for points 1 through 3 indicate how the flow calculated using the ideal gas flow equation is converging for the different segments. Flow at point 4 represents the value of flow at point 1 less the packing-gland flow to the shell of feedwater heater 5. Pressure at point 2 is shell pressure of the governing stage, an important variable for control of the plant feedwater flow.

Points 1 through 8 of the ILPT data represent information at the points shown on Fig. B.2. Exhaust loss is taken from the enthalpy at point 8 before gross electrical output from the ILPT is calculated.

Feedheater state variables are explained as follows; temperatures are in degrees Fahrenheit, enthalpies are in Btu/lbm, and flows are lbm/s. Feedwater heater 4 is a deaerator and is modeled quite differently from the other feedheaters. As such, certain variables are not applicable and are zeroed.

<u>Acronyms</u> (Figs. B.1 and B.2)

TFCO — temperature of feedwater at outlet drain-cooler section [$T_{FC,\phi}$ of Eq. (15)].

TFCA — temperature of feedwater halfway along the drain-cooler section [$T_{FC,A}$ of Eq. (16)].

TFEO — temperature of feedwater at the outlet of the evaporator section [$T_{FE,\phi}$ of Eq. (17)].

TFEA — temperature of feedwater halfway along evaporator section [$T_{FE,A}$ of Eq. (18)].

TDCO — temperature of liquid at the drain-cooler outlet [$T_{DC,\phi}$ of Eq. (19)].

TDCA — temperature of liquid halfway along drain-cooler section [$T_{DC,A}$ of Eq. (20)].

TFHV — saturated vapor temperature in the feedwater heater shell [T_V of Eq. (23)].

TFWO — temperature of feedwater at the outlet of the feedwater heater. Differences between TFWO and TFEO represent amount of superheat in the shell inlet vapor flow.

TFWI — temperature of feedwater at the inlet of the feedheater.

TFHI — temperature of liquid in the evaporator section [T_ℓ of Eq. (20)]. As mentioned in the text, this variable should not rise significantly above TFHV. If it does, flashing of this liquid into steam is occurring and must be accounted for, which requires modifying differential equations.

WFHC — vapor condensing rate in the feedheater shell [W_c of Eq. (14)].

WDVI — vapor flashing rate of previous drain-cooler liquid [$W_{DC,f}$ of Eq. (12)].

WFHV — saturated vapor flow into the feedwater heater shell [W_v of Eq. (10)].

WFHL — saturated liquid flow into the feedwater heater shell [W_ℓ of Eq. (10)].

WDLI — previous drain-cooler liquid flow rate [$W_{DC,\ell}$ of Eq. (12)].

WFW — feedwater flow rate out of feedheater.

WDC — total drain-cooler outlet flow rate.

TFEI — temperature of feedwater at the evaporator section inlet.

HFWI — enthalpy of feedwater at the feedwater inlet.

HFEI — enthalpy of feedwater at the evaporator section inlet.

HFEO — enthalpy of feedwater at the evaporator section outlet.

HFWO — enthalpy of feedwater at the feedheater outlet.

HDCI — enthalpy of drain-cooler liquid at the drain-cooler section inlet [$h_{DC,i}$ of Eq. (13)].

HDCO — enthalpy of drain-cooler liquid at the drain-cooler section outlet.

HFHV — saturated vapor enthalpy at shell pressure [h_v of Eq. (11)].

HFHS — enthalpy of turbine extraction steam [h_s of Eq. (11)].

WFHS — turbine extraction steam flow rate [W_s of Eq. (11)].

PFHV — saturation pressure of shell.

User's note on stability: There is a timestep between the printed values of WFHS and WFHV. At a given transient time, these values should be approximately the same for dry extraction steam. If a significant difference exists between the two printed values, a numerical oscillation may be occurring. In such a case, either the timestep should be reduced or vapor holdup time (HFVH) increased.

NUREG/CR-1789
ORNL/NUREG/TM-399
Dist. Category R8

Internal Distribution

1. S. J. Ball
2. K. W. Childs
3. J. C. Cleveland
4-8. J. C. Conklin
9. J. G. Delene
10. L. C. Fuller
11. P. R. Kasten
12. W. A Miller
13. F. R. Mynatt
14. J. L. Rich
15. J. P. Sanders
16. R. S. Stone
17. T. K. Stovall
18. H. E. Trammell
19. ORNL Patent Office
20. Central Research Library
21. Document Reference Section
22-23. Laboratory Records Department
24. Laboratory Records (RC)

External Distribution

25-28. Director, Office of Nuclear Regulatory Research, USNRC, Washington, D.C. 20555
29. Chief, Experimental Gas-Cooled Reactor Safety Research Branch, Division of Reactor Safety Research, Office of Nuclear Regulatory Research, USNRC, Washington, DC 20555
30. Director, Reactor Division, DOE, ORO, Oak Ridge, TN 37830
31. Office of Assistant Manager for Energy Research and Development, DOE, ORO, Oak Ridge, TN 37830
32-33. Technical Information Center, DOE, Oak Ridge, TN 37830
34-333. Given distribution as shown in category R8 (10 — NTIS)